Increased beat-to-beat variability of cerebral microcirculatory perfusion during atrial fibrillation: a near-infrared spectroscopy study

Increased beat-to-beat variability of cerebral microcirculatory perfusion during atrial fibrillation: a near-infrared spectroscopy study.

Andrea Saglietto, MD[1#], Stefania Scarsoglio, Prof[2#], Daniela Canova[1], PhD, Silvestro Roatta[3], Prof, Nefer Gianotto, MD[1], Alessandro Piccotti[1], Simone Franzin[2], Fiorenzo Gaita, MD Prof.[4], Gaetano Maria De Ferrari, MD Prof.[1], Luca Ridolfi, Prof.[5], Matteo Anselmino, MD Prof.[1]

[1] Division of Cardiology, "Città della Salute e della Scienza di Torino" Hospital, Department of Medical Sciences, University of Turin, Turin, Italy;
[2] Department of Mechanical and Aerospace Engineering, Politecnico di Torino, Turin, Italy;
[3] Department of Physiology, University of Turin, Turin, Italy;
[4] Cardiovascular Department, Clinica Pinna Pintor, Policlinico di Monza, Turin, Italy;
[5] Department of Environmental, Land and Infrastructure Engineering, Politecnico di Torino, Turin, Italy.

[#]These authors contributed equally.

*Corresponding author: Matteo Anselmino; email address: matteo.anselmino@unito.it; address: Corso Dogliotti 14, Torino; telephone number: (39)-0116709598

Word count: 4180

Conflict of interests: none

Data availability statement: data available on request

Abstract

Aims: Atrial fibrillation (AFib) is associated with cognitive decline/dementia, independently from clinical stroke/transient ischemic attack (TIA). Recent *in silico* data suggested that AFib could induce transient critical hemodynamic events in cerebral microcirculation. Our aim was to use non-invasive spatially resolved cerebral near-infrared spectroscopy (SRS-NIRS) to investigate *in vivo* beat-to-beat microcirculatory perfusion and after sinus rhythm (SR) restoration.

Methods: Cerebral SRS-NIRS with high-frequency sampling (20 Hz) and non-invasive systemic hemodynamic monitoring were performed before and after elective electrical cardioversion (ECV) for AFib/atrial flutter (AFL). To assess beat-to-beat effects of the rhythm status, the frequency distribution of inter-beat differences in tissue hemoglobin index (THI), a proxy of microcirculatory cerebral perfusion, was compared before and after SR restoration.

Results: 53 AFib/AFL patients (mean age 69±8 years, 79% males) were ultimately enrolled. Cardioversion was successful in restoring SR in 51 (96%) patients. In front of a non-significant decrease in arterial blood pressure variability between pre- and post-ECV measurements, a significant decrease of both extreme hypoperfusive and hyperperfusive/hypertensive microcirculatory events was observed after SR restoration ($p < 0.001$ and $p = 0.041$, respectively).

Conclusion: The present is the first *in vivo* demonstration that SR restoration by ECV significantly reduces the burden of extreme single-beat hemodynamic events in cerebral microcirculation of AFib patients. Future studies are needed to assess whether SR maintenance might slow the long-term cognitive burden of AFib.

Keywords: near-infrared spectroscopy; cerebral microcirculation; atrial fibrillation

Introduction

Atrial fibrillation (AFib) prevalence, currently settled at 1-4% worldwide, is rapidly rising, and is expected to double by 2050.

On top of an increased risk of ischemic stroke, AFib causes cognitive decline and dementia[1,2]. Different mechanisms have been proposed to explain the stroke-independent association between AFib and dementia, such as silent brain lesions (silent cerebral infarction, white matter lesions and cerebral microbleeds)[3–5], chronic reduction in mean cerebral blood flow[6], inflammation[7] and cerebral vascular dysfunction[8–10]. In addition, computational simulations suggest that AFib directly induces beat-to-beat effects on cerebral microcirculation, provoking transient critical hypoperfusions or hypertensive events, typically of a single-beat duration[11,12]. However, an *in vivo* validation of these computational findings is presently lacking, mostly due to the limitations of the currently adopted non-invasive techniques assessing cerebral hemodynamics (transcranial Doppler [TCD] and cerebral arterial spin labelling perfusion magnetic resonance imaging [ALS-MRI])[13,14], which cannot provide a beat-to-beat assessment of microcirculatory dynamics.

Recently, spatially resolved near-infrared spectroscopy (SRS-NIRS), a non-invasive technique mainly used to monitor cerebral tissue oxygenation in critical care, has shown the ability to provide non-invasive insights on cerebral microcirculation with high temporal resolution, sensitive to beat-to-beat variations[15].

Aim of the present study is to monitor cerebral microcirculatory perfusion by SRS-NIRS to detect if occurrence of critical hemodynamic events is reduced after sinus rhythm (SR) restoration by electrical cardioversion (ECV).

Methods

Consecutive patients scheduled for electrical ECV in our Center were screened from January to August 2019 for study inclusion. Given common co-existence and clinical management[16], AFib and atrial flutter (AFL) patients were both included. Persistent AFib/AFL was defined according to European Society of Cardiology (ESC) guidelines[16]. Exclusion criteria were: first-diagnosed, long-standing persistent (> 1 year duration of the ongoing episode) and permanent AFib; AFib in presence of precipitating factors (sepsis, acute myocardial ischemia, untreated dysthyroidism); severe comorbidities (e.g. hepatic injury – defined as an increase in aminotransferase blood level above the upper reference limit – and renal failure – defined as an estimated glomerular filtration rate less than 30 ml/kg/1.73m^2 by CKD-EPI formula); hemodynamic instability (systolic blood pressure < 90 mmHg, altered consciousness, or reduced peripheral perfusion documented by an increased arterial blood lactate [> 2 mmol/L]); electrolyte abnormalities.

All patients received oral anticoagulation (either vitamin K antagonist – VKA, or direct oral anticoagulant – DOAC), for at least 4 weeks before and after ECV (long-term anticoagulation therapy was then guided by patients' thromboembolic risk profile). For patients on VKA, the level of anticoagulation was considered adequate if international normalized ratio (INR) > 2.0 during 4 weeks before ECV; in case of suboptimal pre-procedural anticoagulation, a transoesophageal echocardiography (TEE) was performed. All patients on DOAC underwent pre-procedural TEE, accordingly to our center protocol. ECV was postponed if thrombi in the left atrium or left atrial appendage were found. Study protocol was approved by the local ethical committee and was conducted according to the principles of the Helsinki Declaration. All subjects gave written informed consent prior to study inclusion.

Cardioversion and monitoring

Anaesthesia was induced by propofol (standard dose 1 mg/kg, titrated according to patient response).

If necessary, oxygen supplementation was delivered by the anesthesiologist through a bag mask valve. Once deep sedation was achieved, ECV was performed by delivering up to three synchronized direct-current biphasic shocks adopting a step-up protocol (from 200 to 360 J). ECV was considered successful in case of sinus rhythm restoration.

Detailed description of SRS-NIRS can be found elsewhere[17]. Briefly, NIRS is an optical technique based on near-infrared light that allows quantifying changes in tissue concentration of intravascular oxygenated and deoxygenated haemoglobin. Since NIRS signals, despite being mainly sensitive to microvasculature changes, may be affected by extra-cranial blood sources, SRS-NIRS has been implemented to minimize the influence of extra-cerebral circulation on NIRS measurements. In particular, tissue haemoglobin index (THI), a SRS-NIRS parameter that measures tissue total haemoglobin concentration (in arbitrary units), reflects local changes in cerebral tissue blood volume (assuming a constant haematocrit), indirectly providing an index of local microvascular perfusion (see Supplementary Materials for further details). For the present analysis, SRS-NIRS monitoring was recorded with the patient in supine position by using a two-channel NIRO-200NX monitor (Hamamatsu Photonics K.K.) placing the probes of each channel on left and right side of patient's forehead, 1 cm above the eyebrow (Supplementary Figure 1). Each probe consisted of a pulsed laser emitter diode and a detector with 3 sensors, with an emitter-detector distance of 4 cm. NIRS probes were left in place throughout the whole procedure, as well as room temperature was kept constant (20-23°C), guarantying comparability between pre- and post-ECV measurements.

Continuous non-invasive measurement of arterial blood pressure (ABP) was performed by a photo-plethysmographic system applied to the right middle finger (CNAP Monitor 500AT-HD, CNSystems Medizintechnik AG), while oxygen saturation (SpO_2) was simultaneously and continuously measured with pulse oximetry (Capnostream^{TM} 20p, Medtronic). Continuous electrocardiographic monitoring was recorded (Dynascope Monitor, DS-7100, Fukuda Denshi Co. Ltd), and a twelve-lead electrocardiogram printed before and after the procedure to document cardiac rhythm (MyCardioPad^{XL}, Esaote).

NIRS signals from both channels were digitally acquired with the highest sampling frequency available (20 Hz) by a proprietary software (N200NXOL, Hamamatsu Photonics K.K.), while all other signals were simultaneously acquired using the Micro1401-3 multichannel data acquisition system and Spike2 software (Cambridge Electronic Design Limited). The average lengths of pre- and post-ECV NIRS signals were 4764 ± 1420 s and 2918 ± 699 s, respectively. The number of recorded heartbeats was 5733 ± 2023 in pre-ECV and 3045 ± 875 in post-ECV, comparable to those simulated in computational models[11,12].

Signal post-processing

THI-NIRS signals were visually inspected and movement artefacts or disturbances in the form of spikes and discontinuities were excluded from the analysis. In this way, only regular signal segments were extracted from raw measures. No substantial differences emerged between the two channels. For each patient, we selected the least noisy channel, taking into account that: (i) the beat-to-beat information of the THI signal was as distinguishable as possible; (ii) the whole signal was smooth over as many continuous temporal ranges as possible, without showing artifacts and jumps. As signals exhibit low-frequency fluctuations (due to respiration and/or occasional patient or eye movements), that prevent continuous-time signal analyses, these segments were then aligned in order to have the overall average equal to one. An example of the signal shifting procedure is reported in Supplementary Figure 2. Then, the corresponding synchronous ABP and electrocardiographic signals were identified. Using the electrocardiographic data to detect RR beats boundaries, the succession of beat-averaged values (μ_i) for THI and ABP was evaluated; subscript *i* refers to the *i*-th beat. Due to the high sampling frequency (20 Hz for THI and 400 Hz for ABP), several values of THI (and ABP) were recorded in each beat. μ_i is obtained by averaging these values over the beat, thus μ_i is equal to the mean value of the THI (and ABP) signal evaluated over the i-th beat. In order to highlight beat-to-beat variations, the following variable is then introduced:

$$N_i = \frac{\mu_i - \mu_{i+1}}{\mu_i} \qquad (1)$$

Positive (negative) values of the variable N_i mark beats where the beat-averaged value of the THI and ABP signal decreases (increases) in the next beat. In the definition (1), the division by μ_i is introduced to evaluate beat-to-beat changes in relative terms and to provide a dimensionless variable. The division by μ_i allows us to capture the weight of the change of the beat-averaged mean. N_i represents an indicator of first-difference between beat-averaged values, which better highlights beat-to-beat variations rather than the mean values reached in each beat.

In order to detect relevant beat-to-beat variations, we used the fourth moment of the frequency distribution of the variable N_i. For each of the THI and ABP signals (for example, the THI measured under pre-cardioversion conditions), the beat-to-beat distribution of the N_i values is obtained; then, the distance (N_i -$\overline{N}$) of each value N_i from the mean value $\overline{N}$ of the time series is evaluated (Figure 1); finally, the fourth moment for each patient is evaluated as

$$m_4(N) = \frac{1}{M}\sum_i (N_i - \overline{N})^4 \qquad (2)$$

where M is the number of beats considered in the summation. The high value of the exponent (the fourth power) is chosen to weigh more the tails of the N_i distribution, i.e. the extreme values. In other words, given two signals, if the first has a statistically significant higher m_4 than the second signal, it means that the first signal more often reaches extremely high (or low) values with respect to its average than the second does. The 4th moment is the typical statistical metric used to focus on extreme events, being variance (sensitive to the core of probability distribution) less effective, and odd moments (e.g. 3rd , 5th) sensitive to the difference in sign. m_4 is thus obtained by exploiting the whole RR distribution, that is all the M beats of each patient. The occurrence of extreme hypo- or hyper-perfusion events is not imposed, but appears when high m_4 values are reached. In order to distinguish hypo-perfusion and hyper-perfusion events – that fall in the right and left tails of the distribution, respectively – the fourth moment is evaluated separately for the two tails, that is, considering in the summation of equation (2) either only the positive differences or only the negative ones. In this way, we can define a fourth moment related to hypoperfusion events (right tail, m_4^r; Figure 1) and a fourth

moment related to hypertensive events (left tail, m_4^l; Figure 1).

Statistical analysis

Continuous data are reported as mean (± standard deviation) or median (interquartile), in case of non-Gaussian distribution; categorical data are reported as absolute number (percentage). Paired t-test was performed to compare RR intervals, mean THI and mean ABP values before and after ECV. Wilcoxon signed ranked test was performed to assess intra-patient variations of the right (m_4^r) and the left (m_4^l) fourth moments of the probability distribution of inter-beat THI and ABP variability before and after ECV. Benjamini-Hochberg procedure was used to adjust p-values for multiple comparisons. A sensitivity analysis separately assessing patients with AFib and patients with AFL was performed. Quintile regression analysis using the difference between pre- and post-ECV fourth moment of inter-beat THI variability as the dependent variable was performed to assess predictors of the intracerebral signal variability reduction. In addition, we also computed the coefficients of determination (R^2), for the log-log pre- and post-ECV THI values.

All analyses were performed using R software version 3.3.0 (R Foundation for Statistical Computing, Vienna, Austria). A p-value of 0.05 was considered statistically significant.

Results

71 patients referred to our Center for AFib/AFL ECV were screened for possible inclusion in the study; according to inclusion criteria, 53 patients were ultimately enrolled. A detailed description of the reasons for study exclusion can be found in the Supplementary Material. Table 1 reports baseline clinical characteristics of the included subjects. Mean age was 69 ± 8 years, with a male predominance (79%). Nearly all the patients (92%) were on anti-arrhythmic drug therapy. Cardioversion was successful in 51 patients (96%), with a mean of 1.15 ± 0.45 shocks per patient. All patients remained hemodynamically stable, no additional airway management was necessary and no procedural complications occurred.

Complete signal processing was feasible on 44 out of the 53 patients enrolled: 5 patients were excluded due to low-quality NIRS signals, 2 due to active cardiac stimulation of a permanent pacemaker, 2 for ECV failure in restoring sinus rhythm. Pre- and post-ECV RR intervals were respectively 0.85±0.14 s and 0.99 ± 0.14 s ($p < 0.001$). Pre- and post-ECV mean THI values were 0.99 ± 0.05 and 1.05 ± 0.30 ($p = 0.266$), while corresponding mean ABP values were 93.9 ± 11.6 mmHg and 89.3 ± 11.4 mmHg, respectively ($p = 0.001$). A statistically significant decrease both in m_4^r and m_4^l of inter-beat THI variability was observed after sinus rhythm restoration ($p < 0.001$ and $p = 0.041$, respectively; Table 2). Conversely, we did not find differences concerning m_4^r and m_4^l of inter-beat ABP variability between pre- and post-ECV ($p = 0.283$ and $p = 0.400$, respectively; Table 2).

At quintile regression analysis, internal carotid artery stenosis was the sole clinical parameter significantly associated with a greater reduction in beat-to-beat signal variability reduction ($p = 0.02$ for m_4^l; please refer to Supplementary Table 1 for complete regression analysis data).

A sensitivity analysis was also performed stratifying, based on the twelve-lead electrocardiogram registered before the procedure, within AFib (31, 70%) and AFL patients (13, 30%). Figure 2 shows 10-seconds segments of pre- and post-ECV THI and ABP recordings for two patients, the first with

AFib (panel A) and the second with AFL (panel B). Statistically significant decrease both in m_4^r and m_4^l after sinus rhythm restoration was observed in patients with AFib ($p < 0.001$ and $p = 0.026$, respectively), while no significant differences were observed in AFL patients (Table 3). m_4^r reached higher inter-beat THI variability values than m_4^l in both AFib and AFL patients (Tables 2 and 3). Despite a trend towards decrease, no significant differences were found concerning m_4^r and m_4^l of inter-beat ABP variability before and after successful ECV, both in AFib and in AFL patients (AFib: $p = 0.208$ and $p = 0.240$; AFL: $p = 0.382$ and $p = 0.650$, respectively; Table 3).

The scatter-plots of pre- and post-ECV m_4^r and m_4^l of inter-beat THI variability are reported in Figure 3, stratified by arrhythmia type.

Discussion

In the present study we have assessed beat-to-beat hemodynamic signals of the cerebral circulation in AFib/AFL patients, before and after sinus rhythm restoration by ECV, with the use of SRS-NIRS at a high sampling frequency (20 Hz).

The main findings are:

- Sinus rhythm restoration significantly reduced the burden of extreme single-beat hemodynamic events in cerebral microcirculation;
- Despite a trend towards reduction, extreme single-beat ABP events did not vary significantly before and after ECV.

The present data support the computational hypothesis that hemodynamic alterations related to the "irregularly irregular" AFib rhythm, although being relatively absorbed at the systemic level (ABP signal) thanks to short-term regulation feedbacks, are not dampen along the cerebrovascular circulation, and result in an increased burden of extreme single-beat hemodynamic events at the microcirculatory level. The inter-beat THI variability, representative of perfusion variations in the cerebral microcirculation, significantly varied after cardioversion, while the inter-beat ABP variability only showed a non-significant trend towards reduction (Table 3), highlighting a bigger impact of AFib-induced perturbations on the distal cerebral circulation compared to the systemic district. It can be speculated that this behaviour might be a consequence of different dynamics (latency and/or gain) in short-term feedback mechanisms between the systemic circulation (baroreceptors) and the inner cerebral circle (cerebral autoregulation mechanism), as well as mechanical and structural properties of the complex network of brain vessels, resulting in proximal-to-distal amplification of AFib-related hemodynamic perturbations along the cerebral circulation. Moreover, a recent work by Junejo et al.[9] demonstrated for the first time that individuals with AFib present a diminished cerebral autoregulation compared both to healthy controls and hypertensive patients without AFib. In this regard, it is also noteworthy that a greater benefit of the ECV, in terms of reduction of cerebral

microcirculatory extreme events probability, was seen in patients with internal carotid artery stenosis, a condition known to reduce cerebral autoregulation efficiency[18]. However, future dedicated studies are needed to test this explanatory hypothesis. In addition, the sensitivity analysis, based on accurate pre-ECV rhythm assessment, strengthens the hypothesis that the reduction in the burden of extreme hemodynamic events in cerebral microcirculation is mainly driven by the elimination of a highly irregular rhythm. In fact, we did not observe differences in terms of extreme events before and after SR restoration in case of AFL, an atrial arrhythmia considered and managed equally to AFib, but characterized by a less irregular ventricular response. These observations support the hypothesis that "irregularly irregular" systemic hemodynamic perturbations exerted by AFib, due to its irregular RR intervals, constitutes a critical issue challenging cerebral autoregulation system.

Our data integrate recent evidences in the field of cerebral hemodynamics during AFib. Using ALS-MRI before and after AFib cardioversion, Gardarsdottir et al.[19] demonstrated that successful SR restoration, maintained for at least 10 weeks, related to a significant increase in cerebral perfusion (+4.9 ml/100g/min). Despite the limited temporal resolution of ALS-MRI not permitting to assess beat-to-beat variations in perfusion, this is an elegant demonstration that successful cardioversion in AFib patients increases the *mean* cerebral distal perfusion. Wutzler et al.[20], using non-spatially resolved NIRS monitoring with very low frequency sampling (< 1 Hz), reported an increase in *mean* cerebral oxygen saturation (indirectly reflecting cerebral perfusion) after successful cardioversion. Thanks to the high temporal resolution of the cerebral SRS-NIRS at maximum frequency sampling (20 Hz), the present study focuses on extreme *beat-to-beat* hemodynamic events at the level of cerebral microcirculation. Taken together, these data suggest that AFib exerts detrimental effects on cerebral hemodynamics both by lowering mean cerebral perfusion, likely due to the absence of atrial kick during ongoing arrhythmia, and by inducing transient beat-to-beat perfusion perturbations which are perpetuated up to cerebral microcirculatory level, due to RR intervals irregularity.

To our knowledge, the present is the first *in vivo* demonstration of AFib-induced beat-to-beat alterations in cerebral microcirculation, supporting the hypothesis that AFib *per se* may promote

cognitive dysfunction and dementia through a chronic occurrence of extreme hemodynamic events.

Limitations

First, sample size limits multivariate analysis aiming to correlate the fourth moment of inter-beat THI variability to baseline clinical characteristics and prescribed medications. Second, although post-ECV sampling has been acquired after recovery from deep sedation, it cannot be excluded that an anaesthetic "tail" might impact post-ECV measurements. In this regard, the lack of a non-cardioversion control group and day test re-test reproducibility measures constitute a limitation of the present study. Third, limited sample size of AFL patients may have not provide sufficient power to detect significant differences in THI signals in the sensitivity analysis. Finally, even though the SRS-NIRS algorithm is designed to reduce extra-cranial circulation influence, it cannot be excluded that a residual impact might be present, possibly affecting THI measurements.

Conclusions

The present is the first *in vivo* demonstration that sinus rhythm restoration by ECV, significantly reduces, in AFib patients, the burden of extreme single-beat hemodynamic events in cerebral microcirculation. Future studies are needed to confirm a direct causal relationship and to investigate whether sinus rhythm maintenance with modern rhythm control strategies, such as catheter ablation, might reduce the long-term cognitive burden in AFib patients.

Acknowledgments

This study was performed thanks to the support of the "Compagnia di San Paolo" (https://www.compagniadisanpaolo.it) granted to MA within the project "Progetti di Ricerca di Ateneo–2016: Cerebral hemodynamics during atrial fibrillation (CSTO 60444)" of the University of Turin, Italy. The funders had no role in study design, data collection and analysis, decision to publish, or preparation of the manuscript.

We would also like to thank patients, Prof. Mauro Rinaldi and Elisabetta Toso for participating at the study. We also thank Ivan Ferrandino for helping in the setting-up of the recordings. Special mention goes to Antonietta Carfora, Elena Maria Richiardi, Anna Renzetti, Prof. Enrico Lupia, Prof. Luca Brazzi (for his group of Anesthesiologists), and Antonio Ferraro (for his group of Professional Nurses) for actively promoting the study.

References

1. Dagres N, Chao TF, Fenelon G, Aguinaga L, Benhayon D, Benjamin EJ, *et al.* European Heart RhythmAssociation (EHRA)/Heart RhythmSociety (HRS)/Asia Pacific Heart RhythmSociety (APHRS)/LatinAmerican Heart RhythmSociety (LAHRS) expert consensus on arrhythmias and cognitive function: What is the best practice? *Europace* Oxford University Press; 2018;**20**:1399–400.
2. Saglietto A, Matta M, Gaita F, Jacobs V, Bunch TJ, Anselmino M. Stroke-independent contribution of atrial fibrillation to dementia: A meta-analysis. *Open Hear* BMJ Publishing Group; 2019;**6**.
3. Gaita F, Corsinovi L, Anselmino M, Raimondo C, Pianelli M, Toso E, *et al.* Prevalence of silent cerebral ischemia in paroxysmal and persistent atrial fibrillation and correlation with cognitive function. *J Am Coll Cardiol* J Am Coll Cardiol; 2013;**62**:1990–7.
4. Selim M, Diener HC. Atrial fibrillation and microbleeds. Stroke. Lippincott Williams and Wilkins; 2017. p. 2660–4.
5. Conen D, Rodondi N, Müller A, Beer JH, Ammann P, Moschovitis G, *et al.* Relationships of Overt and Silent Brain Lesions With Cognitive Function in Patients With Atrial Fibrillation. *J Am Coll Cardiol* Elsevier USA; 2019;**73**:989–99.
6. Gardarsdottir M, Sigurdsson S, Aspelund T, Rokita H, Launer LJ, Gudnason V, *et al.* Atrial fibrillation is associated with decreased total cerebral blood flow and brain perfusion. *Europace* Oxford University Press; 2018;**20**:1252–8.
7. Aldrugh S, Sardana M, Henninger N, Saczynski JS, McManus DD. Atrial fibrillation, cognition and dementia: A review. J. Cardiovasc. Electrophysiol. Blackwell Publishing Inc.; 2017. p. 958–65.
8. Junejo RT, Braz ID, Lucas SJE, Lieshout JJ van, Lip GYH, Fisher JP. Impaired Cerebrovascular Reactivity in Patients With Atrial Fibrillation. J. Am. Coll. Cardiol. Elsevier USA; 2019. p. 1230–2.
9. Junejo RT, Braz ID, Lucas SJE, Lieshout JJ van, Phillips AA, Lip GYH, *et al.* Neurovascular coupling and cerebral autoregulation in atrial fibrillation. *J Cereb Blood Flow Metab* SAGE Publications Ltd; 2020;**40**:1647–57.
10. Junejo RT, Lip GYH, Fisher JP. Cerebrovascular Dysfunction in Atrial Fibrillation. Front. Physiol. Frontiers Media S.A.; 2020.
11. Anselmino M, Scarsoglio S, Saglietto A, Gaita F, Ridolfi L. Transient cerebral hypoperfusion and hypertensive events during atrial fibrillation: A plausible mechanism for cognitive impairment. *Sci Rep* Nature Publishing Group; 2016;**6**.
12. Saglietto A, Scarsoglio S, Ridolfi L, Gaita F, Anselmino M. Higher ventricular rate during atrial fibrillation relates to increased cerebral hypoperfusions and hypertensive events. *Sci Rep* Nature Publishing Group; 2019;**9**.
13. Naqvi J, Yap KH, Ahmad G, Ghosh J. Transcranial Doppler ultrasound: A review of the physical principles and major applications in critical care. Int. J. Vasc. Med. Int J Vasc Med; 2013.
14. Deibler AR, Pollock JM, Kraft RA, Tan H, Burdette JH, Maldjian JA. Arterial spin-labeling in routine clinical practice, part 1: Technique and artifacts. Am. J. Neuroradiol. AJNR Am J Neuroradiol; 2008. p. 1228–34.
15. Saglietto A, Scarsoglio S, Ridolfi L, Canova D, Anselmino M. Cerebral spatially resolved near-infrared spectroscopy (SRS-NIRS): paving the way for non-invasive assessment of cerebral hemodynamics during atrial fibrillation. *Minerva Cardioangiol* 2020;
16. Hindricks G, Potpara T, Dagres N, Arbelo E, Bax JJ, Blomström-Lundqvist C, *et al.* 2020 ESC Guidelines for the diagnosis and management of atrial fibrillation developed in collaboration with the European Association of Cardio-Thoracic Surgery (EACTS): The

Task Force for the diagnosis and management of atrial fibrillation of the European. *Eur Heart J* 2020;

17. Suzuki S, Takasaki S, Ozaki T, Kobayashi Y. Tissue oxygenation monitor using NIR spatially resolved spectroscopy. *Optical Tomography and Spectroscopy of Tissue III* 1999.
18. White RP, Markus HS. Impaired dynamic cerebral autoregulation in carotid artery stenosis. *Stroke* Lippincott Williams and Wilkins; 1997;**28**:1340–4.
19. Gardarsdottir M, Sigurdsson S, Aspelund T, Gardarsdottir VA, Forsberg L, Gudnason V, *et al.* Improved brain perfusion after electrical cardioversion of atrial fibrillation. *Europace* Oxford University Press; 2020;**22**:530–7.
20. Wutzler A, Nee J, Boldt LH, Kühnle Y, Gräser S, Schröder T, *et al.* Improvement of cerebral oxygen saturation after successful electrical cardioversion of atrial fibrillation. *Europace* Europace; 2014;**16**:189–94.

Figure Legends

Figure 1. For each signal, the beat-to-beat distribution of the N_i values is obtained; then, the distance (N_i -$\bar{N}$) of each value N_i from the mean value $\bar{N}$ of the time series is evaluated. The high value of the exponent (the fourth power) is chosen to weigh more the tails of the N_i distribution, i.e. the extreme values. In order to distinguish events that fall in the right and left tails of the distribution, respectively, the fourth moment is evaluated separately for the two tails.

Figure 2. Example of pre-cardioversion synchronous time series of ECG, THI and ABP signals during atrial fibrillation (left panel, patient #3) and atrial flutter (right panel, patient #24). Notice (i) the very good correspondence between ECG, THI and ABP signals and (ii) the remarkable decrease of the THI signal when a long beat occurs during atrial fibrillation.

Figure 3. Scatter-plots of pre- and post-ECV m_4^r and m_4^l of inter-beat THI variability, stratified by arrhythmia type (lower panels). Coefficients of determination, R^2, for the log-log pre- post- ECV relations are: 0.59 for m_4^l AFib; 0.49 for m_4^l AFL; 0.49 for m_4^r AFib; 0.34 for m_4^r AFL. Upper panels show two time series of THI signals during atrial fibrillation and after sinus rhythm restoration (patient #3).

Tables

Table 1. Baseline characteristics of the patients enrolled (N=53), also stratified by arrhythmia type.

Variables	Total (N = 53)	AFib (N = 39)	AFL (N = 14)
Age (years)	69 ± 8	69 ± 9	69 ± 10
Male sex	42 (79%)	32 (82%)	10 (72%)
BMI (kg/m^2)	27.0 ± 3.7	27.3 ± 3.5	26.4 ± 4.5
Hypertension	44 (83%)	32 (82%)	12 (86%)
Diabetes	5 (9%)	5 (13%)	0 (0%)
Previous stroke/TIA	5 (9%)	5 (13%)	0 (0%)
Supra-aortic trunks stenosis	6 (11%)	6 (15%)	0 (0%)
EHRA class			
Class I	30 (57%)	21 (54%)	9 (64%)
Class II	20 (38%)	15 (38%)	5 (36%)
Class III	3 (6%)	3 (8%)	0 (0%)
Heart failure	5 (9%)	4 (10%)	1 (7%)
Coronary artery disease	2 (4%)	2 (5%)	0 (0%)
CHA_2DS_2-VASc score	2.5 ± 1.5	2.6 ± 1.5	2.2 ± 1.3
HAS-BLED score	1.6 ± 1.0	1.6 ± 1.0	1.4 ± 1.0
Cardiac implantable device	2 (4%)	2 (5%)	0 (0%)
Echocardiographic parameters			
Left ventricular ejection fraction (%)	58 ± 6	58 ± 6	58 ± 7
Indexed left atrial volume (ml/m^2)	50 ± 15	51 ± 16	46 ± 11
End-diastolic left ventricular diameter (mm)	49 ± 6	50 ± 6	46 ± 7
Medications			
Amiodarone	14 (26%)	14 (36%)	0 (0%)
Class IC	28 (53%)	19 (49%)	9 (64%)
Sotalol	7 (13%)	5 (13%)	2 (14%)
Beta-blocker	38 (72%)	27 (69%)	11 (79%)
Digoxin	6 (11%)	4 (10%)	2 (14%)
Aspirin	2 (4%)	2 (5%)	0 (0%)
VKA	12 (23%)	10 (26%)	2 (14%)
DOAC	41 (77%)	29 (74%)	12 (86%)

AFib, atrial fibrillation; AFL, atrial flutter; BMI, body mass index; DOAC, direct oral anticoagulant; TIA, transient ischemic attack; VKA, vitamin K antagonist.

Table 2. Pre- and post-ECV values of the fourth moment (m_4^r and m_4^l) of the probability distribution of inter-beat THI and ABP variability.

	Pre-ECV	**Post-ECV**	p-value	Adjusted p-value*
Inter-beat THI variability (right tail, m_4^r)	$5.96*10^{-9}$ [$7.80*10^{-10}$; $1.07*10^{-8}$]	$1.34*10^{-9}$ [$3.70*10^{-10}$; $4.43*10^{-9}$]	<0.001	**<0.001**
Inter-beat THI variability (left tail, m_4^l)	$3.04*10^{-9}$ [$6.75*10^{-10}$; $6.81*10^{-9}$]	$1.04*10^{-9}$ [$3.89*10^{-10}$; $3.51*10^{-9}$]	0.041	**0.041**
Inter-beat ABP variability (right tail, m_4^r)	$3.21*10^{4}$ [$2.54*10^{3}$; $6.92*10^{4}$]	$2.12*10^{4}$ [$1.50*10^{3}$; $9.12*10^{4}$]	0.283	0.283
Inter-beat ABP variability (left tail, m_4^l)	$1.72*10^{4}$ [$3.52*10^{3}$; $4.57*10^{4}$]	$2.41*10^{3}$ [$3.87*10^{2}$; $3.35*10^{4}$]	0.200	0.400

Values are reported as median [interquartile range]. P-values are derived by Wilcoxon signed rank test. *Benjamini-Hochberg adjusted p-value (multiple comparison testing)

Table 3. Sensitivity analysis of pre- and post-ECV values of the fourth moment (m_4^r and m_4^l) of the probability distribution of inter-beat THI and ABP variability according to atrial arrhythmia (AFib or AFL).

	Pre-ECV	**Post-ECV**	p-value	Adjusted p-value*
Atrial fibrillation (n = 31)				
Inter-beat THI variability (right tail, m_4^r)	$7.41*10^{-9}$ [$2.26*10^{-9}$; $2.04*10^{-8}$]	$1.94*10^{-9}$ [$4.32*10^{-10}$; $6.79*10^{-9}$]	**<0.001**	**<0.001**
Inter-beat THI variability (left tail, m_4^l)	$4.33*10^{-9}$ [$1.03*10^{-9}$; $1.10*10^{-8}$]	$1.30*10^{-9}$ [$5.24*10^{-10}$; $5.37*10^{-9}$]	**0.047**	**0.047**
Inter-beat ABP variability (right tail, m_4^r)	$3.40*10^{4}$ [$2.62*10^{3}$; $6.53*10^{4}$]	$3.46*10^{4}$ [$6.90*10^{3}$; $9.64*10^{4}$]	0.104	0.208
Inter-beat ABP variability (left tail, m_4^l)	$1.68*10^{4}$ [$4.42*10^{3}$; $3.43*10^{4}$]	$2.52*10^{3}$ [$3.72*10^{2}$; $6.41*10^{4}$]	0.240	0.240
Atrial flutter (n = 13)				
Inter-beat THI variability (right tail, m_4^r)	$1.25*10^{-9}$ [$3.63*10^{-10}$; $5.94*10^{-9}$]	$6.51*10^{-10}$ [$1.94*10^{-10}$; $1.46*10^{-9}$]	0.248	0.496
Inter-beat THI variability (left tail, m_4^l)	$1.12*10^{-9}$ [$3.10*10^{-10}$; $2.95*10^{-9}$]	$5.71*10^{-10}$ [$2.41*10^{-10}$; $1.17*10^{-9}$]	0.650	0.650
Inter-beat ABP variability (right tail, m_4^r)	$3.16*10^{4}$ [$2.30*10^{3}$; $7.31*10^{4}$]	$1.02*10^{3}$ [$4.72*10^{2}$; $8.59*10^{4}$]	0.382	0.764
Inter-beat ABP variability (left tail, m_4^l)	$3.04*10^{4}$ [$2.63*10^{3}$; $4.95*10^{4}$]	$1.10*10^{3}$ [$4.03*10^{2}$; $2.20*10^{4}$]	0.650	0.650

Values are reported as median [interquartile range]. P-values are derived by Wilcoxon signed rank test. *Benjamini-Hochberg adjusted p-value (multiple comparison testing)

Figure 1.

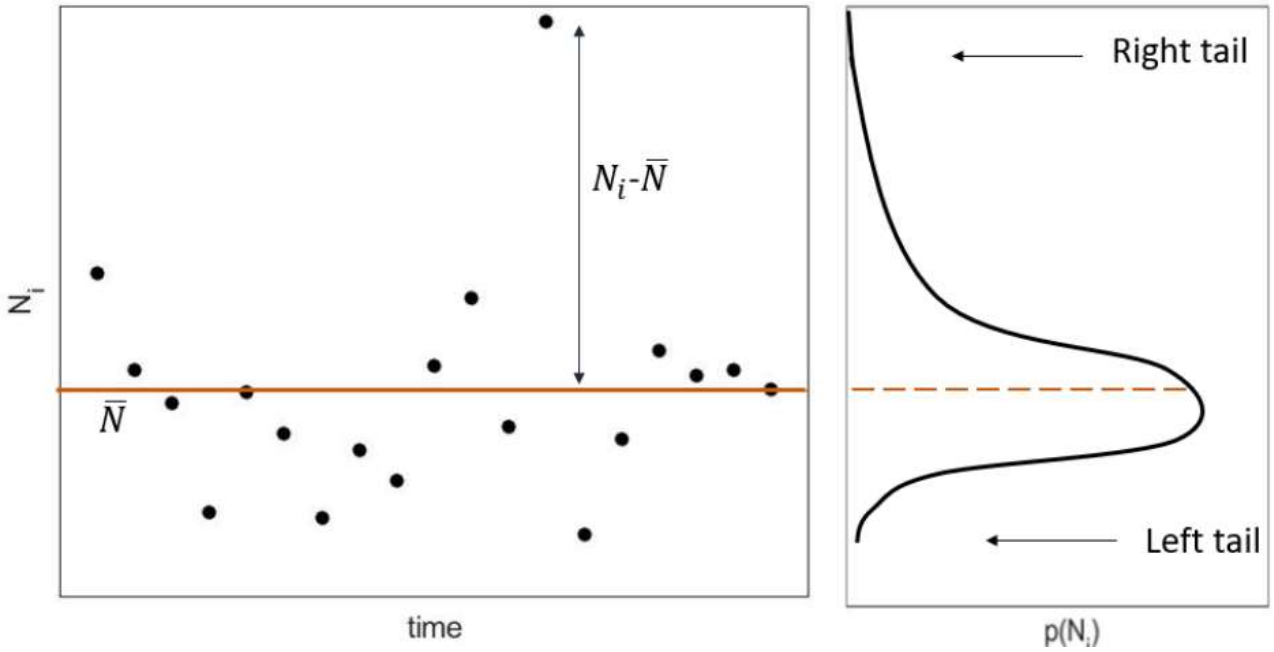

Figure 2.

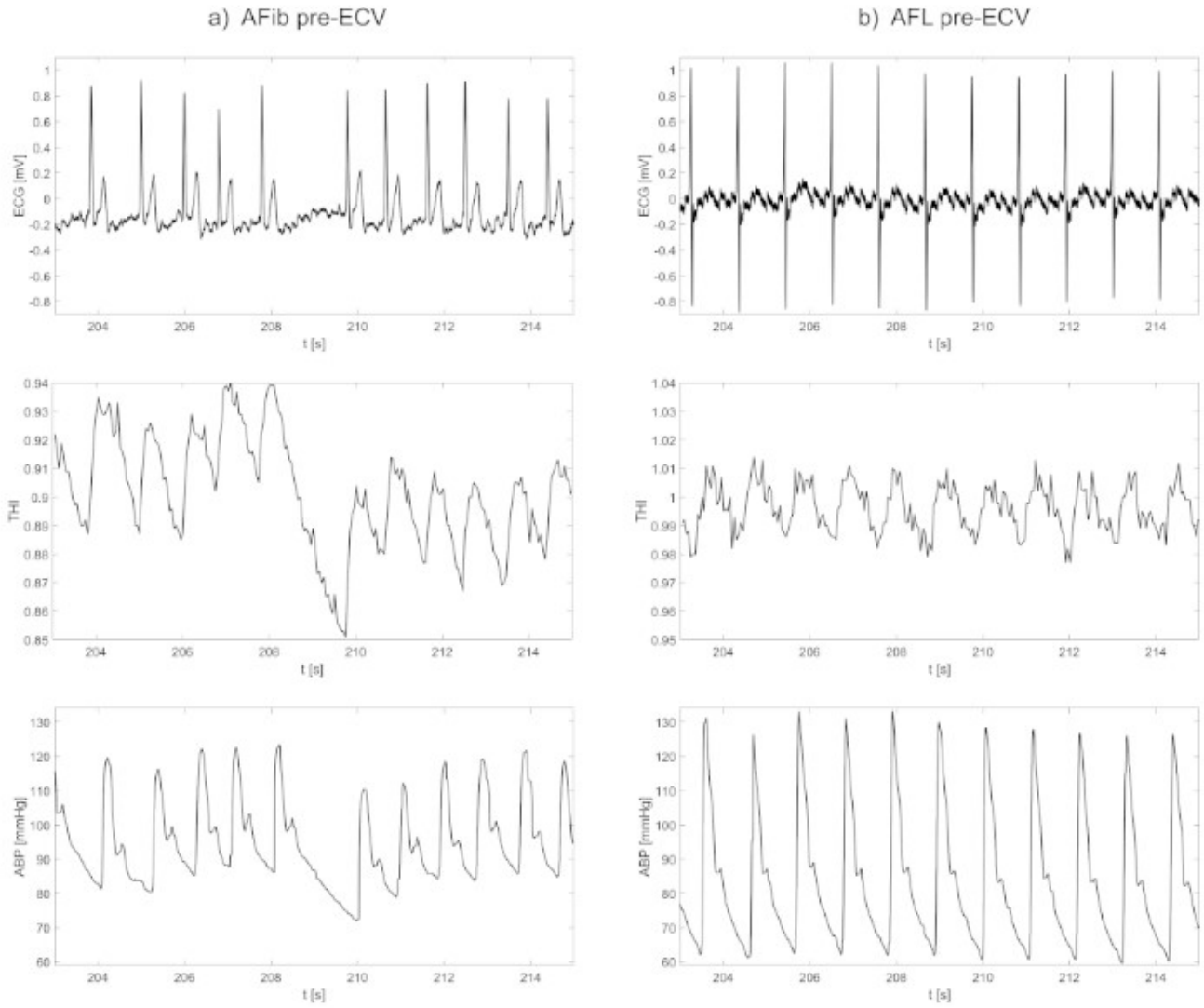

Figure 3.

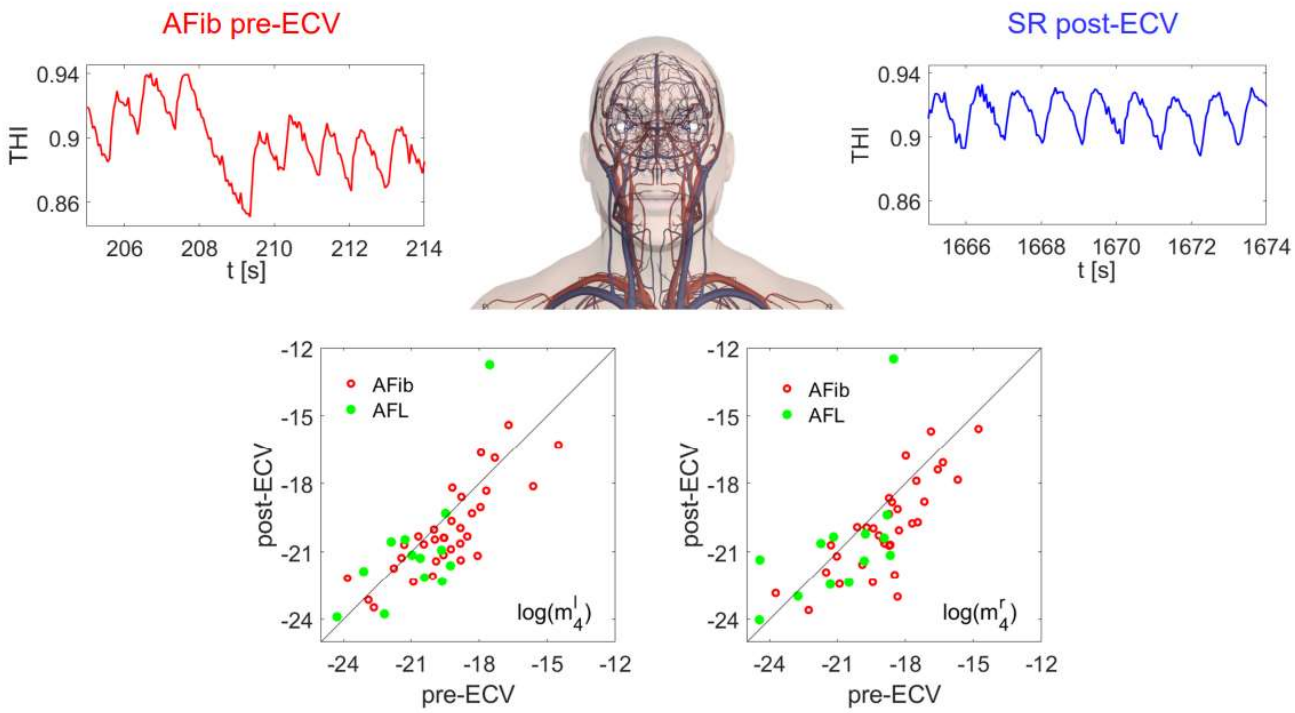
AFib pre-ECV
SR post-ECV
THI
0.94
0.9
0.86
206
208
210
212
214
1666
1668
1670
1672
1674
t [s]
AFib
AFL
post-ECV
pre-ECV
-12
-15
-18
-21
-24
log(m$_4^l$)
log(m$_4^r$)